ANZIAM J. 50(2009), 283–305
doi:10.1017/S1446181109000224

NUMERICAL DETERMINATION OF CRITICAL CONDITIONS FOR THERMAL IGNITION

W. LUO[1], G. C. WAKE✉[1] and C. W. HAWK[2]

(Received 15 September, 2008; revised 15 December, 2008)

Abstract

Ignition or thermal explosion in an oxidizing porous body of material can be described by a dimensionless reaction–diffusion equation of the form $\partial_t u = \nabla^2 u + \lambda e^{-1/u}$. Here such equations will be formulated in symmetrically shaped bounded regions Ω, effectively reducing the mathematical formulation to that of one dimension. This is critically re-examined from a modern perspective using numerical methods. A computer algorithm is constructed and used to carry out a broad-ranging evaluation of the watershed critical initial temperature conditions for thermal ignition of nonuniform assemblies. It is then shown how the resulting mathematical structure for the ignition threshold curves can be correlated by a hyperbolic conic section with a high degree of accuracy over the full range of positive ambient temperature values. However, this sometimes over-predicts (which is bad) and sometimes under-predicts (which is good) the critical initial condition. The definition of additional dimensionless parameters is found to generate further simplification, leading to a universal correlating form capable of collapsing the entire solution space onto a single line in the plane of the new variables. In addition, this study considers the physically intuitive conjecture that spatial moments of the initial temperature profile ought to possess a direct mathematical link to the critical ignition threshold. As such, the mth-order spatial moment of the critical total energy content integrals is defined, and an empirical result is derived stating that certain orders of this moment should be insensitive to changes in ambient temperature and initial shape profile and may be considered functionally dependent on the dimensionless eigenvalue only, within some quantifiable error band. Spatial moment integrals, based on computed critical threshold conditions, are found to support this conjecture, with the best accuracy obtained for the second-order moments.

2000 *Mathematics subject classification*: primary 80A25; secondary 35K55.
Keywords and phrases: thresholds for ignition, blow-up, computation.

[1]Institute of Information & Mathematical Sciences, Massey University, Auckland, New Zealand; e-mail: g.c.wake@massey.ac.nz, weiwei_luo@yahoo.com.
[2]University of Alabama in Huntsville, Alabama, USA (deceased).

1. Introduction

Ignition or thermal explosion of a combustible substance occurs when exothermic reactions evolve heat so rapidly that it is impossible to preserve a stable balance between heat production and heat loss to the surroundings. The archetypal example of self-heating is a porous pile of material in which heat is internally generated by atmospheric oxidation. If the excess heat in the pile can be transported and dissipated to the surroundings fast enough, an equilibrium or steady state can be safely established. Under certain conditions, however, the dissipation mechanism cannot keep pace with the self-heating rate and spontaneous ignition or explosion will occur. These critical conditions depend on the size and shape of the pile, the assembly temperature of the material, and the ambient temperature of the surrounding environment.

The basic theoretical construct for this problem may be erected in a rather straightforward manner using conservation principles and well-established descriptions of the underlying chemical and physical processes. The resulting mathematical formulation is commonly referred to as the reaction–diffusion equation (only the energy balance):

$$\rho c_p \frac{\partial T}{\partial t} = \nabla.(k\nabla T) + H(T),$$

where t is time, T is the absolute temperature, ρ is the density, c_p is the specific heat, k is the thermal conductivity, and $H(T)$ is the rate of heat production per unit volume at temperature T. This nonlinear partial differential equation is a localized expression of the conservation of energy and implies that the rate of change of thermal energy within a unit volume element is equal to the net conduction heat transfer through the bounding surface plus the volumetric heat generation rate.

For most ignition problems of practical importance, it is possible to incorporate certain simplifying assumptions which make the mathematics more tractable. These include: (1) negligible reactant consumption, diffusion and advection (that is, the so-called "zero-order" reaction); (2) constant thermal conductivity; and (3) Arrhenius temperature dependence for exothermic reaction rate.

Use of these assumptions yields the following working form for the nonlinear heat conduction equation:

$$\alpha \frac{\partial T}{\partial t} = \nabla^2 T + \frac{\rho Q A}{k} e^{-E_a/RT}, \tag{1.1}$$

where $\alpha = \rho c_p/k$ is the reciprocal of the thermal diffusivity, Q is the heat of reaction per unit mass (that is, the "exothermicity"), A is the pre-exponential frequency factor in the Arrhenius reaction rate term, E_a is the activation energy, and R is the universal gas constant; see Bowes [3]. When applied over a bounded region Ω, equating the heat flux on the boundary to that of the net radiation of energy to the surroundings (linearized by use of the approximation embodied in Newtonian cooling) yields a mixed boundary condition on the piecewise smooth surface $\partial\Omega$,

$$k \frac{\partial T}{\partial n} = h(T_a - T_s), \tag{1.2a}$$

https://doi.org/10.1017/S1446181109000224 Published online by Cambridge University Press

where $\partial/\partial n$ is the outward normal derivative on $\partial\Omega$, h is the convective heat transfer coefficient, T_a is the ambient temperature of the surrounding environment, and T_s is the material surface temperature. In order to make the full problem well posed, we need an initial condition

$$T(x, 0) = T_0(x) \quad \text{on } \partial\Omega \text{ and its boundary.} \tag{1.2b}$$

Given the shape and size of a bounded region, appropriate boundary conditions, and values for the fundamental material properties, the basic objective is to mathematically exploit the reaction–diffusion equation and determine the critical parameters and conditions leading to the onset of ignition or thermal explosion. In particular, we are concerned with predictions for the critical ambient temperature, which defines an external environmental constraint for safe "storage", and the critical initial temperature, which defines an internal constraint for safe "assembly".

From a mathematical perspective, there are two fundamental strategies for attacking the reaction–diffusion equation and determining critical conditions for thermal ignition. These are the stationary (steady-state) model and the nonstationary (transient) model.

In the stationary model, the time-dependent term in Equation (1.1) is neglected and steady-state solutions are sought for which heat losses exactly balance heat production. This approach assumes unlimited reactants and implies that either a small steady-state excess temperature will become established in the body or conversely that the temperature will increase rapidly to a much higher temperature (the upper steady-state) well above that which is sustainable in practical situations. The principal attraction of the stationary modelling approach is a reduction of the problem to a more amenable ordinary differential equation form, which has facilitated the development and refinement of standard mathematical methods capable of accounting for internal spatial temperature distributions and producing reliable estimates for the critical ambient temperature. Because the stationary model cannot account for time evolution, however, it has only limited effectiveness in the prediction of critical initial conditions. It is well known, for instance, that many fires have resulted from the assembly of reactive material at too high an initial temperature even though the storage conditions were subcritical on the basis of steady-state theory; see, for example, Bowes [3] (who refers to this as thermal explosion of the second kind), Rivers *et al.* [7], and Smedley and Wake [8].

The nonstationary model, on the other hand, retains the complete time-dependent form of the reaction–diffusion equation and evolves the full temperature history of the self-heating body. The drawback of this approach is the general need to resort to numerical analysis and the fact that a full development history must be computed for each initial/boundary condition of potential interest. The distinct advantage, however, is that it can fully account for the initial assembly conditions and is therefore able to provide accurate estimates for the critical initial temperature. Weber *et al.* [9], for instance, recently conducted a limited computational study of the nonstationary model which clearly demonstrated that the practical critical assembly temperature may, under certain circumstances, be 5–10% lower than the critical temperature

https://doi.org/10.1017/S1446181109000224 Published online by Cambridge University Press

obtained from steady-state theory. This has profound industrial implications in the assessment of fire hazards and the definition of fire safety standards where a clear distinction must be drawn between the classic "storage" problem, where only steady-state temperatures are important, and the less recognized "assembly" problem, where the initial temperature threshold for self-ignition is of vital concern.

The central objective of this research is the development and use of numerical techniques to investigate the nonstationary solution sets of the full time-dependent nonlinear heat conduction equation subject to a general convective boundary condition, and to determine the critical threshold which distinguishes between initial conditions that evolve to a low-temperature steady-state and those that evolve to a high-temperature steady-state attractor (that is, thermally ignite). This numerical methodology is then used as the basis for a broad-ranging numerical study of the "assembly" problem using a generalized one-parameter power law for the initial temperature profile. It is then shown how these results may be effectively reduced using a simple hyperbolic correlation. Lastly, we demonstrate that certain spatial moment integrals of the critical initial temperature distribution are functionally independent of the ambient temperature and the assembly temperature profile.

2. Numerical models

2.1. Dimensionless form in modern variables Despite its predominance in the literature, the traditional Frank–Kamenetskii grouping of dimensionless variables has the effect of confusing the role of the ambient temperature when, in fact, it is the most practically significant control parameter in the problem definition. To circumvent this difficulty, Burnell *et al*. have suggested an alternative dimensionless grouping with temperature rescaled independently of the ambient temperature [4].

The major distinction in the new grouping is the definition of a dimensionless reactant temperature and a dimensionless ambient temperature that are completely decoupled,

$$u = \frac{RT}{E_a} \quad \text{and} \quad U = \frac{RT_a}{E_a}.$$

As in the classical Frank–Kamenetskii formulation (see [3]), we rescale and normalize the spatial and time coordinates using the previously defined dimensionless variables $\xi = x/L$ and $\tau = t/\alpha L^2$. Then substitution of the dimensionless parameters into the reaction–diffusion equations (1.1), (1.2a) and (1.2b) yields the Burnell–Graham-Eagle–Gray–Wake (see [4]) formulation in the modern compact form

$$\frac{\partial u}{\partial \tau} = \nabla_\xi^2 u + \lambda e^{-1/u} \quad \text{in } \Omega,$$
$$\frac{\partial u}{\partial n} + Bi(u - U) = 0 \quad \text{on } \partial\Omega.$$

Here, λ is a new dimensionless "eigenvalue-like parameter" given by

$$\lambda = \frac{L^2 \rho Q A R}{k E_a}.$$

https://doi.org/10.1017/S1446181109000224 Published online by Cambridge University Press

In contrast with the eigenvalue δ of the Frank–Kamenetskii formulation, λ is decoupled from the ambient temperature. Thus, U is the only parameter dependent on T_a. This makes the reconciliation with experimental data, where T_a is the most common control variable, considerably easier.

The new formulation may also be put in a generalized form applicable to all three principal centrosymmetric solids. We expand the Laplacian operator in Cartesian, cylindrical, and spherical coordinates and observe that these can all be represented in the parameterized form

$$\nabla_\xi^2 u = \frac{\partial^2 u}{\partial \xi^2} + \frac{n}{\xi}\frac{\partial u}{\partial \xi},$$

where n is a geometrically defined parameter. That is, $n = 0$, 1 or 2 for the slab, infinite circular cylinder, and sphere, respectively. Hence, the final working form of the reaction–diffusion equation for class A shapes may be written as

$$\begin{aligned} \frac{\partial u}{\partial \tau} &= \frac{\partial^2 u}{\partial \xi^2} + \frac{n}{\xi}\frac{\partial u}{\partial \xi} + \lambda e^{-1/u} \quad \text{in } \Omega, \\ \frac{\partial u}{\partial \xi} &+ Bi(u - U) = 0 \quad \text{on } \partial\Omega. \end{aligned} \tag{2.1}$$

This arrangement of the reaction–diffusion equation contains no simplifying approximations beyond those previously contained in Equations (1.1), (1.2a) and (1.2b) and is a mathematically equivalent framework for the analysis of stationary and nonstationary models of thermal ignition. Indeed, for numerical analyses, there is no distinct advantage in using the Frank–Kamenetskii variables and it is indeed preferable to utilize the Burnell–Graham-Eagle–Gray–Wake formulation, which provides a more direct link to the physical domain. Thus, all formal developments in this work are based on the latter formulation.

2.2. Stationary model Before embarking on the development of the stationary model and a computational study of the oft neglected but practically important assembly problem, it is first necessary to construct stationary model solutions to provide a frame of reference for proper interpretation of the computed critical initial threshold solutions. The stationary model follows directly from the full reaction–diffusion equation in the limit of infinite time in the form

$$\nabla_\xi^2 + \lambda e^{-1/u} = 0 \quad \text{in } \Omega$$

where the boundary condition defined by Equation (2.1) still applies.

Balakrishnan, in one of the first attempts to utilize the Burnell–Graham-Eagle–Gray–Wake variables, revisited the classic stationary model and carried out extensive numerical analyses of the eigenvalue problem using path-following techniques [1]. This work illuminated the characteristic branch structure in the (u, U) plane, including accurate identification of the critical conditions for the steady "storage problem", which is given in terms of the dimensionless ambient temperature U_{cr}, which is defined

https://doi.org/10.1017/S1446181109000224 Published online by Cambridge University Press

as the first value at which the steady state exhibits "gross parametric sensitivity" to small changes in the control parameter U (that is, at the first transcritical bifurcation on the lower branch). This convincingly demonstrates that these alternative variables provide improved physical clarity and gives a more straightforward interpretation in terms of the ambient temperature control parameter, which is usually easily determined.

Here, rather than following the sophisticated path-following solution methodology outlined by Balakrishnan, we use an alternative simple method whereby the conventional two-point boundary value problem is reformulated as an equivalent initial value problem, seen more correctly as a shooting method, as conceived and described by Billingham [2]. This simplification permits the direct construction of accurate solution branches in the $(u(0), U)$ plane, with U as the bifurcation parameter. A complete description of the methodology and validation of the results is given in Luo [5].

2.3. Nonstationary model A standard numerical solution methodology for the transient reaction–diffusion equation, which is parabolic in time and elliptic in space, was constructed on the basis of second-order central differencing of the spatial derivatives and Crank–Nicholson time integration. The resulting discretization equations were applied at each grid point over the computational domain, and closure was achieved through specification of boundary conditions at the symmetry axis and at the external surface $\partial\Omega$. In this way, time evolution of the full reaction–diffusion equation reduces to the solution of a system of linear algebraic equations over a sequence of discrete time steps. Here, it is advantageous to adopt a linear vector space notation, which allows the system of equations to be compactly expressed by the matrix equation

$$KU^{m+1} + LU^m + M = 0, \tag{2.2}$$

where K, L and M are $N \times N$ square matrices containing numerical coefficients and U is an N-element column vector containing the dependent variable values at the grid points. The superscripts denote temporal indices indicative of evolving time. The general solution of Equation (2.2) at time-step $m + 1$ follows immediately and has the basic form

$$U^{m+1} = K^{-1}\lfloor LU^m - M \rfloor \tag{2.3}$$

where K^{-1} is the matrix inverse of K (being nonsingular). It is noted that this simplified approach has linearized the nonlinear Arrhenius term. This is mitigated by the fact that $e^{-1/u}$ has gradient no greater than $4e^{-2} = 0.54$, and the routine has an in-built adaptive step-size feature which is exercised according to the rate at which the solution is changing. Furthermore, the solution was checked against more complicated algorithms in Luo [5] and found to be in agreement.

Equation (2.3) may be solved by a number of algorithms, but the simplest and most convenient follows from the standard Gaussian elimination procedure. Because the nonzero elements of K align themselves along the central three diagonals of the

https://doi.org/10.1017/S1446181109000224 Published online by Cambridge University Press

matrix, the elimination process turns into particularly simple recurrence sequence. This method is commonly referred to as the TDMA (Tri-Diagonal Matrix Algorithm), a formal derivation of which may be found in standard numerical textbooks (see Patankar [6], for instance).

The numerical methodology for nonstationary thermal ignition was implemented in FORTRAN programming language to enable automated machine processing on a digital computer platform. As a validation measure, comparative baseline calculations were then performed with respect to published solutions in the peer-reviewed literature. For a complete description of the numerical solution methodology and supporting validation calculations, see Luo [5].

3. Critical initial conditions in nonuniform assemblies

Using the nonstationary numerical model, it is possible to undertake a judicious examination of the thermally nonuniform assembly problem, in which the fate of a self-heating material can be strongly dependent on initial conditions. Relevant physical examples include the safety of processed reactive materials when placed into piles or bins while hot and the initiation of explosives by localized hot spots (see below). The central issue at hand is whether the initial temperature excess in the assembly will continue to rise indefinitely or dissipate through conductive transport and Newtonian cooling to the surroundings. Of particular interest to this study is the critical demarcation boundary between those initial conditions serving as an onset to ignition/explosion and those which ultimately decay to a self-extinguishing quench state. For the general case of a nonuniform assembly, the transient solution for the evolved state may be expected to display a marked sensitivity to the spatial concentration of thermal energy at the outset, and criticality will depend on the initial temperature distribution. In this section, we examine such subtle mathematical issues in detail by incorporating a generalized self-consistent treatment of the initial temperature distribution for the nonstationary model, which permits direct comparison of criticality predictions against the stationary model. The use of the formulation here gives rise to practical parameter values which are large for λ ($= 10^4$–10^{12}), and small for u, U ($= 0.01$–0.03). When translated back to the dimensional variables, thermal runaway (a rapid but finite temperature increase) occurs in two to three days for materials like milk powder, coal and so on. In the case of wet wool it was often one to two weeks. Obviously this is dependent on T_a.

3.1. Generalized initial shape profile For clarity, we parameterize the solution space for the computational study by adopting a generalized nonuniform initial temperature distribution having the form

$$u(\xi, 0) = U + Cg(\xi),$$

where U is the dimensionless ambient temperature and C is an arbitrary constant representing the initial perturbative displacement from ambient conditions. The principal objective, given values for U, λ and Bi, is determination of the critical value

https://doi.org/10.1017/S1446181109000224 Published online by Cambridge University Press

for C, denoted by C_{cr}, which defines the watershed threshold between those initial conditions that evolve to an upper steady-state (that is, ignition/explosion) and those that evolve to a self-extinguishing steady-state quench. Every shape function g will have a different value of C_{cr}, reflecting the high dimensionality of the set of critical initial conditions.

The initial shape profile is defined by the one-parameter function

$$\begin{gathered} g(\xi) = A_\epsilon(1-\xi^\epsilon), \quad \epsilon \geq 0, \\ g(\xi) \to 1, \quad \epsilon \to \infty \end{gathered} \tag{3.1}$$

where ϵ is the initial profile shape factor and A_ϵ is a normalization factor for preserving total heat content irrespective of profile shape. With this definition, we anticipate the existence of a family of critical initial condition profiles for each value of the initial shape factor, ϵ. These profiles are reasonably general, since any real data for the initial condition (which is typically very sparse) can be fitted by regression to the best fit using ϵ, with its single degree of freedom. Of course, this is indicative only.

Normalization is achieved through a constraint on the spatial integral of $g(\xi)$ such that it is invariant with ϵ . The value of this integral is taken to be unity for convenience:

$$I = \int_0^1 g(\xi)\, d\xi = 1.$$

Thus, substitution of Equation (3.1) and execution of elementary integration steps yields the following expression for the normalization factor:

$$A_\epsilon = \frac{\epsilon+1}{\epsilon}$$

which clearly demonstrates that A_ϵ must decrease as ϵ increases in order to preserve energy content in the distribution. Normalized initial shape profiles for representative values of the shape factor are shown in Figure 1. These include linear ($\epsilon = 1$), parabolic ($\epsilon = 2$), and uniform ($\epsilon = \infty$) initial temperature distributions for the three principal centrosymmetric solids of interest to this study. The singular case is a point source ($\epsilon = 0$), which gives $g(\xi) = \delta(\xi)$, the Dirac delta function centred on the origin. The corresponding normalization factors are summarized in Table 1.

3.2. Parametric survey The general objective of the analysis is to determine the variation in C_{cr} with U, provided fixed values of λ and Bi, using ϵ as an independent parameter for initial heat concentration. We may reasonably anticipate from physical intuition the following functional dependence: (i) C_{cr} will decrease as U increases; (ii) C_{cr} will decrease as λ increases; and, (iii) C_{cr} will decrease as Bi decreases. It is intuitively obvious, however, that $A_\epsilon C_{cr}$ would better serve as the parameter of choice in defining the critical threshold since A_ϵ exhibits a strong dependence on the value of ϵ. Previous cursory numerical investigation has supported the basic preceding conclusions [9], and the intent here is to buttress this argument with additional computational results. Specifically, we construct critical threshold curves for all three principal centrosymmetric solids over a wide range of values for λ and ϵ.

https://doi.org/10.1017/S1446181109000224 Published online by Cambridge University Press

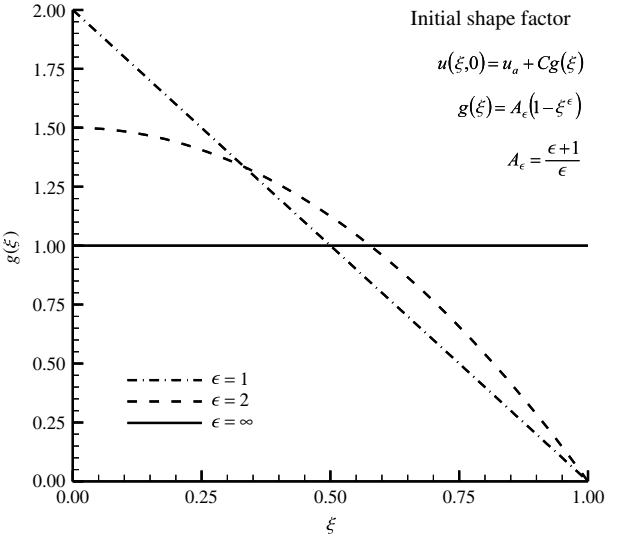

FIGURE 1. Normalized initial shape profiles for representative values of ϵ.

TABLE 1. Summary of profile shape factors and normalization factors.

Profile shape factor (ϵ)	Normalization factor (A_ϵ)
0 (hot spot)	1
1/2	3
1 (linear)	2
2 (parabolic)	3/2
∞ (uniform)	1

To implement the numerical study, it was first necessary to construct an automated search procedure by which the nonstationary model could be used to determine C_{cr} for arbitrary values of U given fixed values for λ, Bi and ϵ. This was accomplished in practice by assuming a very small value for C and computing a fully evolved temporal solution for a selected value of U. If the long-term solution is found to evolve to the lower steady-state solution, the results are recorded, C is given a small incremental increase, and the calculation is automatically repeated again and again. The value of C_{cr} is ultimately resolved when a fully evolved solution to the upper steady-state attractor is obtained. By starting with a very small value for U and repeating the above procedure with incrementally increasing values, it is possible to fully construct the critical initial threshold curve out to the bifurcation point, U_{cr}.

https://doi.org/10.1017/S1446181109000224 Published online by Cambridge University Press

The above automated search procedure was implemented in computer code, and calculations were then carried out for the three principal centrosymmetric solids given $\lambda = 10^4$, 10^6, 10^8 assuming $Bi \to \infty$, which, as mentioned before, are the values found in previous practical investigations: milk powder at the lower end and coal at the higher end. Although this crude search procedure proved effective and accurate for the purpose at hand, it is obviously inefficient and computationally expensive, the exact computing time being dependent, of course, on the size of the step increments and the speed of the microprocessor. In practice, it was necessary to balance the need for fidelity and resolution against the time required to construct a solution. Construction of a single threshold curve of satisfactory accuracy, for instance, would normally take several days of continuous runtime on a dedicated personal computer.

Representative computational results for the nonuniform assembly problem are shown in Figures 2–4, which summarize criticality characteristics for the planar slab, infinite cylinder, and sphere using linear ($\epsilon = 1$), parabolic ($\epsilon = 2$), and uniform ($\epsilon = \infty$) initial temperature distributions. For each value of λ and geometry shape, the critical threshold curves of $u(0) = U + C_{cr}g(0)$ versus U as well as the quench-state curve $u(0)$ versus U are given for each of the three simple geometric configurations under consideration. For purposes of comparison, stable lower and unstable intermediate branch solutions of the stationary model are also displayed on these graphs, the stable lower solution as a continuous line and the unstable ones as dashed lines. The corresponding curves for $A_\epsilon C_{cr}$ versus U are also displayed since they will prove to be important in the analysis to follow. The stable upper steady-state curve is not shown since it is several orders of magnitude larger than the criticality and lower steady-state branches and is of no physical consequence other than serving as a mathematical attractor for ignition.

The mathematical feature of essential importance and interest to be extracted from these results is the fact that the exact criticality threshold, as predicted by the nonstationary model, is significantly different from the unstable intermediate steady state, as predicted by the stationary model. The latter is of course a very weak threshold in the spatially distributed situation discussed here, since upper and lower solutions theory requires the initial condition to be either always above or below this in order to be sure that it will tend asymptotically to the upper or lower stable steady states, respectively. With initial conditions which are neither, the threshold needs to be determined more precisely, as we have shown. Although the models yield identical predictions for the bifurcation point critical ambient temperature, U_{cr}, the ignition threshold for assembly of initially hot materials is found to be considerably lower than that deduced from the stationary model, which of course presumes the initial condition to be always above or below the intermediate steady state(s). This has serious implications, since in the well-stirred reactor the unstable intermediate steady-state solution provides an adequate estimate for safe assembly of potentially hazardous self-heating materials. It is clear from these results, however, that this is severely flawed and its careless use could have grave practical consequences. Interestingly, the intermediate steady state shows that it can both underestimate and overestimate the actual critical threshold, depending on the shape of the initial profile.

https://doi.org/10.1017/S1446181109000224 Published online by Cambridge University Press

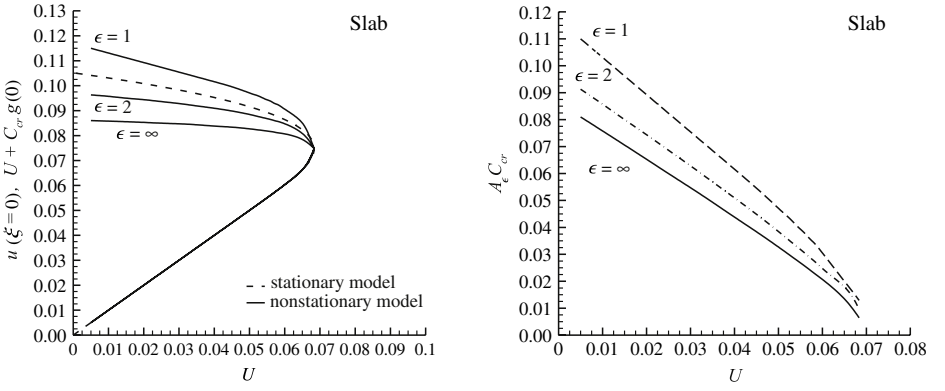

FIGURE 2. Criticality thresholds for nonuniform planar slab assemblies ($\lambda = 10^4$, $Bi = \infty$).

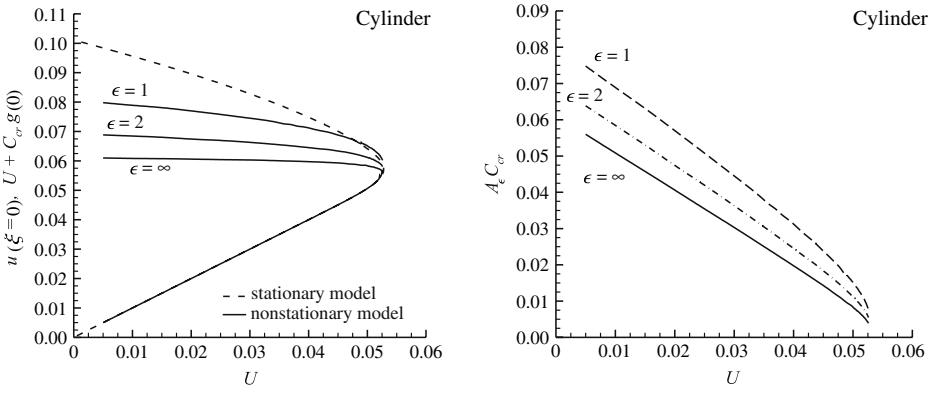

FIGURE 3. Criticality thresholds for nonuniform infinite cylinder assemblies ($\lambda = 10^6$, $Bi = \infty$).

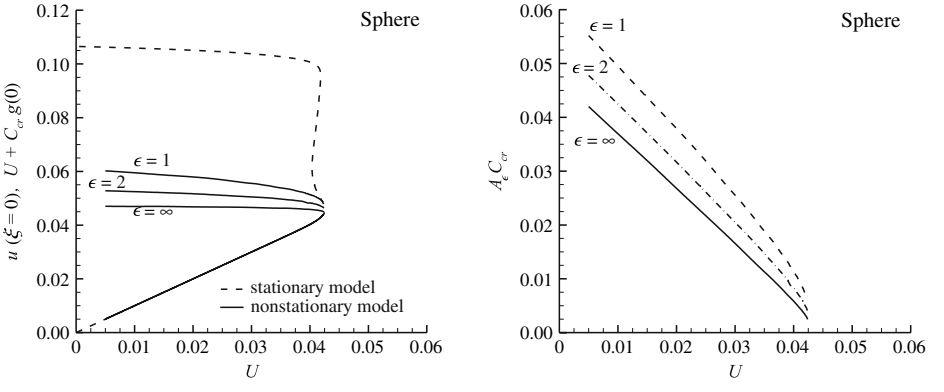

FIGURE 4. Criticality thresholds for nonuniform infinite spherical assemblies ($\lambda = 10^8$, $Bi = \infty$).

https://doi.org/10.1017/S1446181109000224 Published online by Cambridge University Press

4. Correlation and reduction of the critical assembly conditions

The extensive numerical parametric study above was undertaken to identify the critical threshold separating those initial conditions which lead to ignition/explosion and those which ultimately decay to a self-extinguishing quench state. The outcome, a broad set of numerically constructed ignition thresholds over a wide range of values for the dimensionless eigenvalue, provides a reliable database for precisely determining ignition hazards given very specific physical conditions. From a deeper theoretical perspective, however, there is a natural desire to seek further means of reducing, ordering and correlating these results such that the underlying mathematical structure may be revealed and expressed in the most compact and economical form possible.

4.1. Hyperbolic correlation At this stage, we are confronted with a large parametric database for which there are no obvious means of ordering and reducing the results in a straightforward deductive way. What we are seeking, of course, is a means of discovering and revealing hidden mathematical structure through an indirect process of intuitive reasoning. Under these circumstances, it is natural to examine the data in search of basic mathematical forms that can organize the results and provide improved insight. Of the numerous correlating forms that could be considered, conic sections offer one of the simplest and most widely useful constructs available. Here, we examine in detail the application of a second-degree conic section correlation to the critical initial condition thresholds, and demonstrate effective compaction of the solution space's mathematical structure.

Close examination of the threshold curves in the AC_{cr}, U plane reveals structural features which tend to be associated with a hyperbolic conic section. For instance, a hyperbola has a pair of slant asymptotes which approximate the asymptotic behaviour of the critical threshold curves as U decreases towards zero.

In order to develop the desired hyperbolic correlation for the threshold curves in the AC_{cr}, U plane, we begin by noting that a point (x, y) is on the hyperbola with centre (h, k), horizontal vertices $(h, k \pm a)$, and foci $(h, k \pm c)$ if and only if it satisfies the equation

$$\frac{(x-h)^2}{a^2} - \frac{(y-k)^2}{b^2} = 1,$$

where $b^2 = c^2 - a^2$. In this particular case, we identify the transverse and conjugate coordinates in the $A_\epsilon C_{cr}$, U plane as $x = U$ and $y = A_\epsilon C_{cr}$ and define a new parameter $\Gamma = A_\epsilon C_{cr}$ to arrive at the relation

$$\frac{(U-h)^2}{a^2} - \frac{(\Gamma-k)^2}{b^2} = 1.$$

At this point, we impose the obvious constraints $h = U_{cr} + a$ and $k = 0$ and deduce our essential correlation equation

$$\frac{(U-U_{cr}-a)^2}{a^2} - \frac{\Gamma^2}{b^2} = 1. \tag{4.1}$$

https://doi.org/10.1017/S1446181109000224 Published online by Cambridge University Press

Utilization of this correlation equation requires the introduction of certain additional assumptions in order to fully define values for the vertices and the foci. As a basis for the first assumption, we note that the slope of the critical threshold curve $\Gamma = A_\epsilon C_{cr}$ away from the critical ambient temperature, U_{cr}, is approximately unity. Since this slope should match the slope of the slant asymptotes for the hyperbola, which by definition must take the value $\pm b/a$, we immediately deduce the constraint $b \approx a$. In which case, Equation (4.1) takes the simpler form

$$\Gamma_2 = (U - U_{cr} - a)^2 - a^2. \tag{4.2}$$

The final remaining issue concerns definition of the vertex, a. From casual inspection of the critical threshold curves, we clearly anticipate that the value of a must decrease as ϵ increases. As such, we introduce the two-parameter correlating expression

$$a = \alpha + \beta\left(\frac{2}{\epsilon}\right), \tag{4.3}$$

where α and β are fitting parameters and a is assumed to vary inversely with ϵ. Note that a multiplicative factor of 2 was introduced into Equation (4.3) as a means of scaling β such that $a = \alpha + \beta$ when $\epsilon = 2$.

The objective now is to deduce the best parameter values for fitting Equation (4.2) to the precise critical threshold curves in the Γ, U plane based on the complete data set from the preceding parametric study. This exercise yields an array of optimal fitting parameters having a one-to-one correspondence with the array of (n, λ) values from the parametric study. These fitting parameters are summarized in Table 2. Some representative plots of the hyperbolic correlation curves are shown with the precise computational threshold curves in Figure 5 for each value of ϵ. Shown are results for the slab geometry ($n = 0$) with $\lambda = 10^4$, the cylindrical geometry ($n = 1$) with $\lambda = 10^6$ and the spherical geometry ($n = 2$) with $\lambda = 10^8$.

Inspection of these figures clearly demonstrates that the hyperbolic correlation provides an excellent fit to the precise computational results over the full range of ϵ and λ values under consideration. Thus, we conclude that the mathematical structure of the complete solution space is accurately captured by a simple hyperbolic conic section, as defined by Equation (4.2), when using a two-parameter correlating expression for the vertex, as given by Equation (4.3). Variations in the fitting parameters appear to be smooth and well behaved, and it is clear that α and β could further be expressed as analytical functions of n and λ, as well. Here, however, we are content to leave them in tabulated form only.

4.2. Reduction to compact universal form Application of the hyperbolic correlation to the complete parametric solution space provides pleasing results and encourages further examination of the mathematical implications. For example, an immediate follow-on question arises as to whether it is possible to achieve additional reduction through the deduction of a compact universal correlating form. To pursue this question in detail, we revisit our hyperbolic correlation in the simplified form of Equation (4.2).

https://doi.org/10.1017/S1446181109000224 Published online by Cambridge University Press

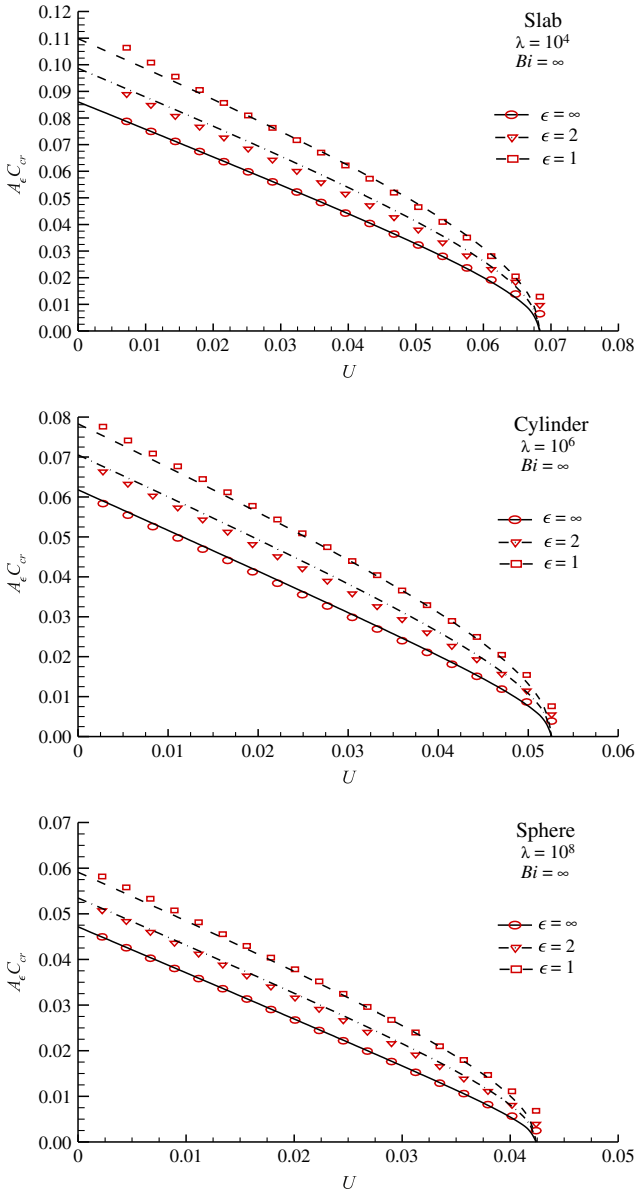

FIGURE 5. $A_\epsilon C_{cr}$ versus U for different assemblies: (top) nonuniform slab assemblies ($\lambda = 10^4$); (middle) nonuniform infinite cylinder assemblies ($\lambda = 10^6$); and (bottom) nonuniform spherical assemblies ($\lambda = 10^8$). Precise computational value – symbols. Hyperbolic correlation – curves.

https://doi.org/10.1017/S1446181109000224 Published online by Cambridge University Press

TABLE 2. Optimal fitting parameters for hyperbolic correlation.

	$\lambda = 10^4$	$\lambda = 10^6$	$\lambda = 10^8$
	Slab ($n = 0$)		
α	0.0200	0.0100	0.0060
β	0.0170	0.0080	0.0052
	Cylinder ($n = 1$)		
α	0.0200	0.0097	0.0056
β	0.0250	0.0110	0.0065
	Sphere ($n = 2$)		
α	0.0200	0.0090	0.0050
β	0.0300	0.0130	0.0075

Our first course of action is to define a new dimensionless temperature $\Delta U = U_{cr} - U$ so that Equation (4.2) may be written as

$$\Gamma^2 = (-\Delta U - a)^2 - a^2.$$

Then we expand the bracketed square in order to find

$$\Gamma^2 = \Delta U^2 + 2a\Delta U \quad \text{or} \quad \Delta U^2 + 2a\Delta U - \Gamma^2 = 0.$$

Noting that this equation is quadratic in ΔU, we may immediately write an expression defining ΔU explicitly in terms of Γ:

$$\Delta U = \sqrt{\Gamma^2 + a^2} - a. \tag{4.4}$$

We now have a convenient explicit correlating form that completely captures the essential mathematical structure of the parametric solution space, and it is strikingly simple. An even simpler form can now be had by defining the right-hand side of (4.4) as a new dimensionless criticality parameter, $\widehat{\Gamma} = \sqrt{\Gamma^2 + a^2} - a$. We therefore arrive at the universal linear correlating form

$$\widehat{\Gamma} = \Delta U.$$

This result is utterly simple and, in a sense, mathematically beautiful since it collapses the entire solution space onto a single line in the $\widehat{\Gamma}$, ΔU plane. The results of this exercise are summarized in Figure 6 for the slab, cylinder and sphere. Although all of the data collapses to the same universal line, the results are depicted separately by geometry in order to avoid excess clutter. We concede that the small errors implicit in this reduction do not give rigorous bounds to the actual threshold, but do give a

https://doi.org/10.1017/S1446181109000224 Published online by Cambridge University Press

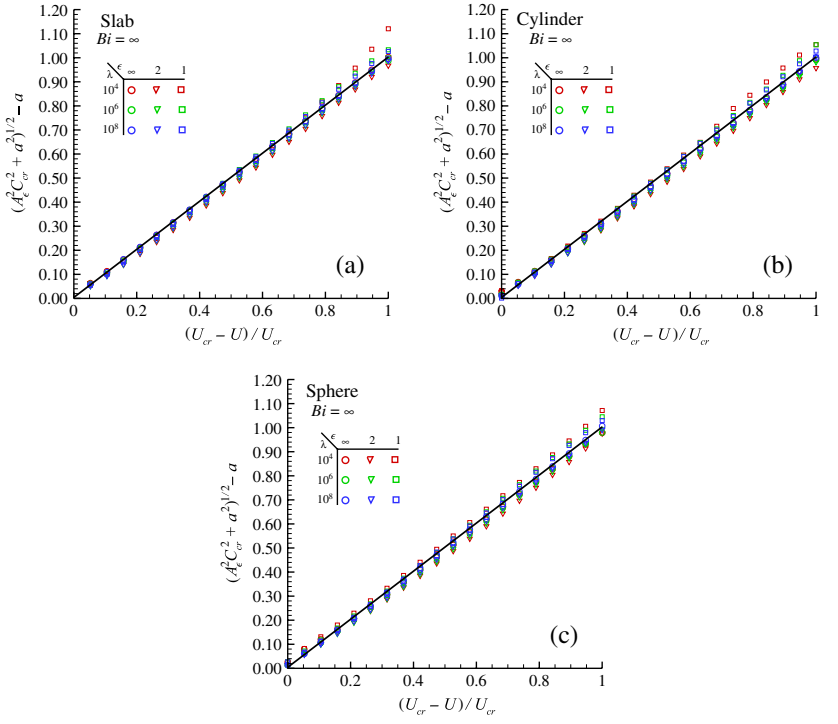

FIGURE 6. Universal correlating line for the three assemblies: (a) infinite slab ($n = 0$); (b) infinite cylinder ($n = 1$) and (c) sphere ($n = 2$).

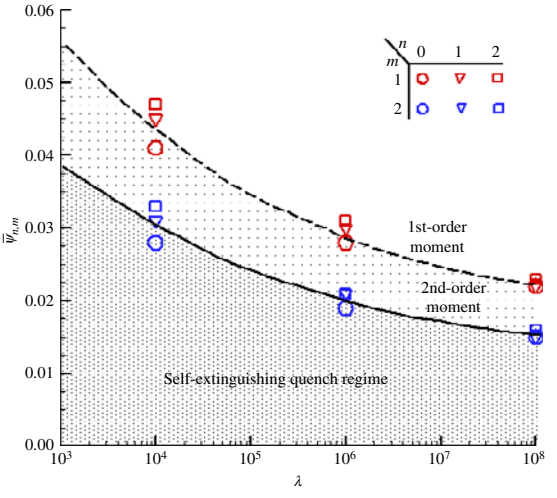

FIGURE 7. Arithmetically averaged values of spatial moment integrals.

https://doi.org/10.1017/S1446181109000224 Published online by Cambridge University Press

way of approximating it. A detailed computation such as outlined earlier is needed if serious doubt remained in any practical instance.

The fit to the universal line is generally good except for some slight deviation in the low ambient temperature region where $U \ll U_{cr}$. This deviation arises from the fact that the actual threshold curve begins to inflect as it nears and passes through the $U = 0$ axis, whereas the hyperbolic correlation requires a continuous merging with the slant asymptote. Even there, the deviation is not extremely large. In general, the fit is better at large values and slightly degrades as the value becomes smaller and the initial thermal distribution has a higher degree of nonuniformity.

4.3. Spatial moments of energy content integral Intuitively, we expect that the ultimate fate of a combustible assembly should have a direct mathematical coupling to its initial energy distribution. We further anticipate that the predisposition for this assembly to either ignite or quench may be conveniently and compactly expressed as an integral over this initial energy distribution. Our purpose, then, is to rigorously define the initial energy content integral and precisely state a mathematical conjecture relating spatial moments of this integral to the fate of thermally nonuniform assemblies of combustible substances. The results of the previous computational parametric study may then used as a basis for thoroughly testing the conjecture and establishing a provisional basis for its acceptance and application to industrial fire problems of great practical interest.

From physical reasoning, we assert that the critical condition for ignition of a thermally nonuniform combustible assembly depends largely upon the initial energy concentration or density, particularly within a centralized hot region as represented by the one-parameter shape profile of Figure 1. Here, the hot spot has been centred on the axis of symmetry as a worst-case representation since the dispersion and removal of excess heat is most impeded under these circumstances.

We begin by noting that the total initial energy content within the material assembly may be expressed succinctly and conveniently as the volume integral of the dimensionless reactant temperature over the complete assembly volume:

$$\hat{E} = \iiint \hat{e}\, dV = \iiint u\, dV.$$

With more specificity, we apply the energy content integral to the principal centrosymmetric solids and obtain the simplified expression

$$\hat{E} = \int_0^1 \hat{e}(\xi, t)\, d\xi = \int_0^1 u(\xi, t)\, d\xi$$

which is to be evaluated at time $t = 0$. As a point of clarification, it should be noted that certain geometrical multiplication factors have been neglected here in order to achieve commonality of form.

https://doi.org/10.1017/S1446181109000224 Published online by Cambridge University Press

Let us proceed further by considering spatial moments of our dimensionless energy content integral. The conventional approach for defining a spatial moment is to weight the kernel of the integral by the distance from the origin (that is, the moment arm) raised to some arbitrary power, which defines the order of the moment. Naturally, this places less weight on contributions to the integral that are closer to the origin than on those that are farther away. Because our hot spot is located on the axis of symmetry, however, we wish to place more weight on integral contributions that are closest to the origin. Thus, we henceforth define our moment arm using the factor $(1 - \xi)$ and define the mth-order spatial moment for the nth class geometry as

$$\psi_{m,n} = \int_0^1 (1 - \xi)^m u(\xi, 0)\, d\xi.$$

Recalling the generalized one-parameter initial shape profile, we deduce the practical working form

$$\psi_{m,n} = \int_0^1 (1 - \xi)^m [U + C_{cr} g(\xi)]\, d\xi = \int_0^1 (1 - \xi)^m [U + C_{cr} A_\varepsilon (1 - \xi^\varepsilon)]\, d\xi. \tag{4.5}$$

It should be clear that this expression is explicitly dependent on the geometrical index n and that the influence of geometry on the spatial moment is carried entirely within the critical constant, C_{cr}.

We now state, based principally on intuitive reasoning, the following mathematical conjecture. *Given any thermally nonuniform assembly in the form of a principal centrosymmetric solid, there exist nonstationary solutions to the Burnell–Graham-Eagle–Gray–Wake reaction–diffusion equation, under the constraint* $Bi \to \infty$, *for which certain order-m spatial moments of the critical total energy content integral,* $\psi_{m,n}$, *are insensitive to changes in the dimensionless ambient temperature,* U, *and the initial shape profile parameter,* ϵ, *and may be considered functionally dependent on the dimensionless eigenvalue,* λ, *only*.

As a means of generating reliable quantitative evidence for the previously stated conjecture, we now consider the first- and second-order spatial moments ($m = 1, 2$) of the critical total energy content integrals over the full parameter space of the computational study. Evaluation of these integrals was effected by numerically integrating (4.5) using a cubic spline interpolation procedure to define $C_{cr} A_\epsilon$ between available data points. The results of these evaluations are summarized in Figures 8–10 which display the variation in $\psi_{m,n}$ with U/U_{cr} over the entire parameter range of the study.

Inspection of the resulting first- and second-order spatial moments provides provisional confirmation of our conjecture and indicates that the second-order moment, which has a narrower error band, may serve as a more accurate basis of prediction. It should also be noted that the error band exhibits a tendency to narrow as the value of λ increases. Results for the third-order spatial moments, which were also computed but not displayed, showed a rewidening of the error band. Apparently,

https://doi.org/10.1017/S1446181109000224 Published online by Cambridge University Press

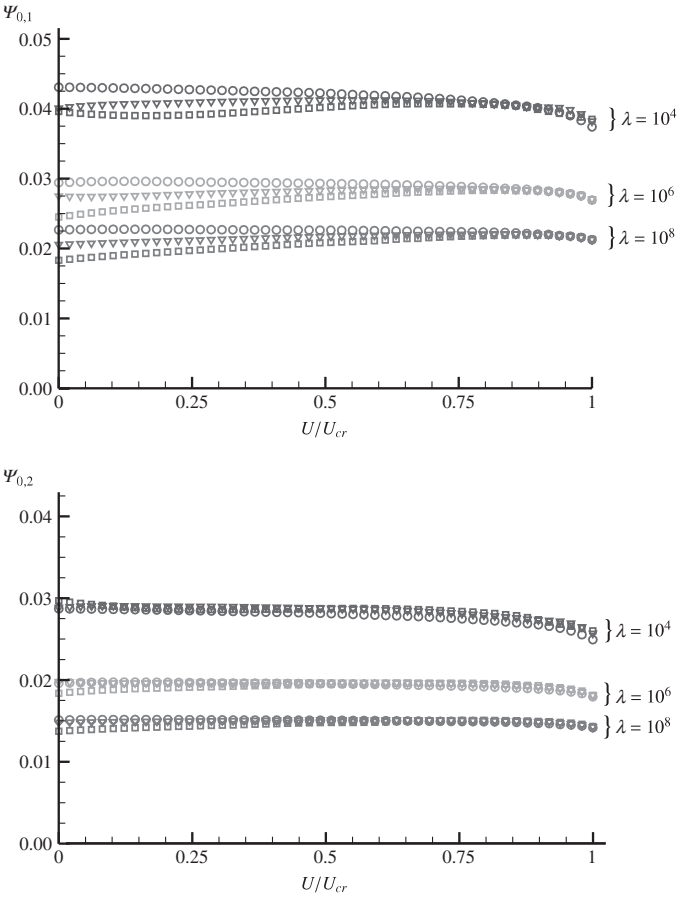

FIGURE 8. Order-m spatial moments of energy content integrals ($n = 0$; $m = 1, 2$). The legend of Figure 6 applies here.

the second-order spatial moment satisfies our conjecture with the least variance and the smallest realizable error band. Spatial moments of noninteger order were not considered.

If we accept these results as provisional validation for the conjecture, we now have at hand a simple method for rapidly calculating fire hazard risks for thermally nonuniform assemblies of self-heating materials. Assuming that the assembly temperature profile $u(\xi, 0)$ is known with a reasonable degree of confidence and that the physical characteristics of the substance are well enough defined to compute λ to good accuracy, one may simply evaluate the spatial moment from (4.5) and compare this result with the mean value of the moments determined by this study. If the computed spatial moment is near or greater than the mean reference value, at the specified value of λ, then the risk of spontaneous ignition should be considered high.

https://doi.org/10.1017/S1446181109000224 Published online by Cambridge University Press

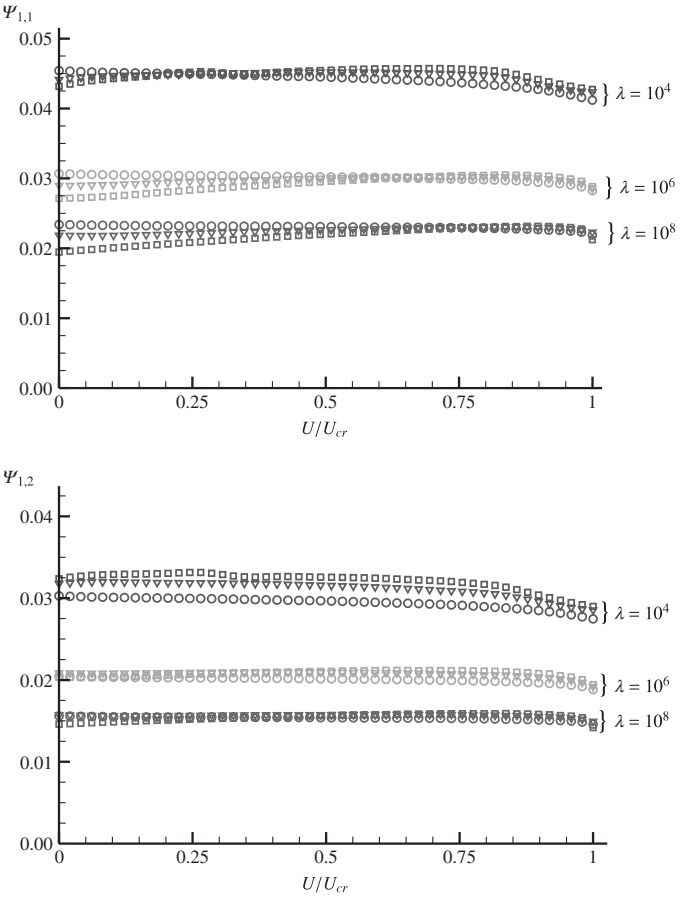

FIGURE 9. Order-m spatial moments of energy content integrals ($n = 1$; $m = 1, 2$). The legend of Figure 6 applies here.

If the computed spatial moment is less than that mean reference value, one may safely assume that the risk is low or negligible, depending on the magnitude of the difference. Arithmetically averaged values for the spatial moment integrals $\overline{\Psi}_{m,n}$ are summarized in Table 3 for convenient utilization and are also plotted as a function of λ in Figure 7.

5. Conclusions

Prior to this work, a number of practically important questions remained unanswered concerning the critical threshold for thermal ignition in reactive assemblies with nonuniform initial temperature distributions. To seek answers to such questions, the reaction–diffusion equation in the dimensionless form $\partial_t u = \nabla^2 u + \lambda e^{-1/u}$ over the bounded region Ω of the principal centrosymmetric solids was critically re-examined from the perspective of modern numerical methodologies.

https://doi.org/10.1017/S1446181109000224 Published online by Cambridge University Press

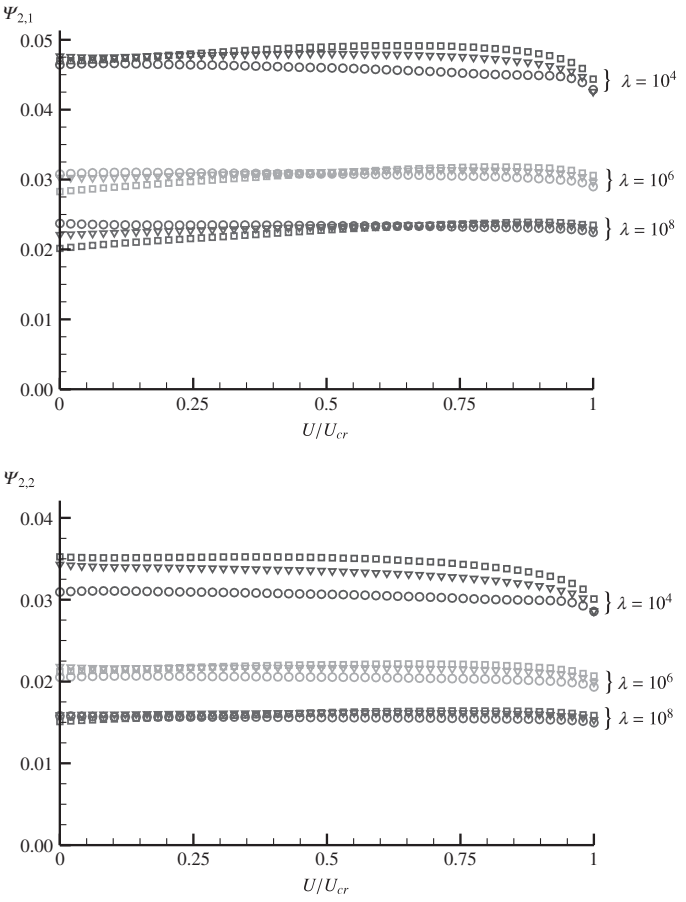

FIGURE 10. Order-m spatial moments of energy content integrals ($n = 2$; $m = 1, 2$). The legend of Figure 6 applies here.

The purpose was to broadly and deeply penetrate the solution space in order to reveal a more detailed description of the underlying mathematical structure, which could be further used to establish conjectural and correlating principles of general predictive utility.

A numerical procedure was then implemented for solving the full time-dependent form of the reaction–diffusion equation. This procedure combined second-order central differencing for the spatial derivative with a Crank–Nicholson time integration scheme, including a time-dependent convective boundary condition, to produce an efficient and accurate solver routine. A judicious examination of the assembly problem was then undertaken to expose how the fate of a self-heating material is dependent on the internal spatial concentration of thermal energy at the time of assembly. By introducing a normalized shape profile for the initial temperature distribution,

https://doi.org/10.1017/S1446181109000224 Published online by Cambridge University Press

TABLE 3. Arithmetically averaged values of spatial moment integrals.

	$\lambda = 10^4$	$\lambda = 10^6$	$\lambda = 10^8$
	Slab ($n = 0$)		
$m = 1$	0.041	0.028	0.022
$m = 2$	0.028	0.019	0.015
	Cylinder ($n = 1$)		
$m = 1$	0.045	0.030	0.022
$m = 2$	0.031	0.021	0.015
	Sphere ($n = 2$)		
$m = 1$	0.047	0.031	0.023
$m = 2$	0.033	0.021	0.016

as defined by a single geometric parameter, it was then possible to compute criticality threshold characteristics over a broad range of practical values for the dimensionless eigenvalue parameter.

It was shown how the resulting mathematical structure for the ignition threshold curves could be correlated by a hyperbolic conic section with a high degree of accuracy over the full range of positive ambient temperature values. Moreover, the clever introduction of new dimensionless parameters within this hyperbolic correlating form was found to generate further simplification, leading to a universal correlating form capable of collapsing the entire solution space onto a single line in the plane of the new variables. This result was found to hold over a wide range of shape parameters and is therefore believed to be of general significance.

In addition, this study addressed the physically realistic conjecture that spatial moments of the initial temperature profile ought to possess a direct mathematical link to the critical ignition threshold. As such, the mth-order spatial moment of the critical total energy content integrals was defined, and a conjecture was formulated stating that certain orders of this moment would remain invariant with changes in ambient temperature and initial shape profile and would therefore be functionally dependent on the dimensionless eigenvalue only, within some quantifiable error band. Evaluations of the spatial moment integrals demonstrated this conjecture to be provisionally valid, with the best accuracy obtained for second-order moments. The invariance property for the spatial moment turns out to be quite powerful and yields a simple but fairly accurate method for estimating fire hazard risks for thermally nonuniform assemblies of self-heating materials. We remark that this was investigated only for profiles of the type given in (3.1). The framing and verification of this conjecture represents a significant accomplishment and greatly expands our mathematical understanding of this practically important problem.

https://doi.org/10.1017/S1446181109000224 Published online by Cambridge University Press

Acknowledgements

Dedicated to the memory of Dr Steve White, who was a fine computational mathematician, and Professor Clark Hawk, of the University of Alabama in Huntsville, who contributed significantly to this work.

References

[1] E. Balakrishnan, "Numerical study of thermal ignition in the new variables", Ph. D. Thesis, Massey University, New Zealand, 1996.
[2] J. Billingham, "Steady-state solutions for strongly exothermic ignition in symmetric geometries", *IMA J. Appl. Math.* **65**(8) (2000) 283–313.
[3] P. C. Bowes, *Self heating: evaluating and controlling the hazards* (Elsevier Science, New York, 1984).
[4] J. G. Burnell, J. G. Graham-Eagle, B. F. Gray and G. C. Wake, "Determination of critical ambient temperatures for thermal ignition", *IMA J. Appl. Math.* **42** (1989) 147–154.
[5] W. Luo, "Numerical determination of critical conditions for thermal ignition", Ph. D. Thesis, Massey University, New Zealand, 2008.
[6] S. V. Patankar, *Numerical heat transfer and fluid flow* (Hemisphere Publishing, New York, 1980).
[7] C. M. Rivers, G. C. Wake and X. D. Chen, "The role of drying in the spontaneous ignition of milk powder", *Math. Eng. Ind.* **6** (1997) 1–14.
[8] S. I. Smedley and G. C. Wake, "Spontaneous ignition: assessment of cause", *Annual Meeting of the Institute of Loss Adjusters of New Zealand*, Palmerston North, NZ, June 1987.
[9] R. O. Weber, E. Balakrishnan and G. C. Wake, "Critical initial conditions for spontaneous thermal ignition", *J. Chem. Soc. Faraday Trans.* **94** (1998) 3613–3617.